J Mater Sci (2011) 46:1602–1605
DOI 10.1007/s10853-010-4971-9

Magnetoelectric performance of cylindrical Ni–lead zirconate titanate–Ni laminated composite synthesized by electroless deposition

W. Wu · K. Bi · Y. G. Wang

Received: 5 July 2010 / Accepted: 30 September 2010 / Published online: 15 October 2010

Abstract The cylindrical Ni–lead zirconate titanate (PZT)–Ni laminated composites with various magnetostrictive–piezoelectric phase thickness ratios were synthesized by electroless deposition. The influences of the bias magnetic field (H_{dc}) and the ac magnetic field frequency (f) on magnetoelectric (ME) effect are discussed. It is seen that the ME voltage coefficient depends strongly on H_{dc} and f. The ME voltage coefficient and electromechanical resonance frequency increase as the magnetostrictive–piezoelectric phase thickness ratio increases. The calculated resonant frequency increases with the magnetostrictive–piezoelectric phase thickness ratio, which agrees well with the experimental results. The maximum ME voltage coefficient of the cylindrical Ni–PZT–Ni laminated composite is 3.256 V cm^{-1} Oe^{-1}, which is much higher than that of the plate laminated composite with the same magnetostrictive–piezoelectric phase thickness ratio. Electroless deposition is an efficient method to prepare ME laminated composites with complex structures. Proper resonant frequency and stronger ME effect can be obtained by optimizing the structure.

Introduction

The magnetoelectric (ME) materials have drawn increasing attention due to their extensive applications such as sensors, actuators, and transducers [1, 2]. The ME effect is characterized by an electric polarization response induced by an applied magnetic field, and/or a magnetization by applying an electric field [3]. Since Astrov [4] discovered the weak ME effect of single crystal Cr_2O_3 in low temperature, many particulate [5–7] and in situ grown [8, 9] ME composites have been developed by combining piezoelectric and magnetostrictive materials. However, due to the limitation of leak current and chemical reactions between phases [1, 10], ME composite did not show strong enough ME effect until Ryu et al. [11] prepared the laminated composite $Tb_{1-x}Dy_xFe_{2-y}$ (Terfenol-D)-Pb(Zr,Ti)O_3 (PZT) with the ME voltage coefficient of 4.68 V cm^{-1}Oe^{-1}.

In the last decade, various investigations [11–15] have been completed to enhance the ME effect by using suitable magnetostrictive and piezoelectric components. The ME voltage coefficient of laminated ME composite can reach a value of 400 V cm^{-1} Oe^{-1} [16]. Besides the inherent properties of magnetostrictive and piezoelectric phases, the magnetic–mechanical–electric coupling influences the performance of laminated ME composite greatly, so the ME voltage coefficient depends on interfacial bonding considerably. Laminated ME composites have been synthesized by several methods such as bonding piezoelectric and magnetostrictive materials together with epoxy and electro-deposition [17–19]. However, the epoxy bonding layer or the electrodes during the process of electro-deposition will reduce the ME coupling [20, 21]. Electroless deposition is believed to be an ideal method for preparing thick functional films with remarkable interfacial bonding [22] and recently we have developed laminated ME composite by electroless deposition [23, 24]. Moreover, it is convenient to prepare thick films on various substrates of complex shapes by electroless deposition.

Wan et al. [25] reported strong flexural resonant ME effect in Terfenol-D/epoxy-PZT bilayers. Pan et al. [26–28] fabricated Ni–PZT–Ni and Ni–PZT cylindrical

W. Wu · K. Bi · Y. G. Wang (✉)
College of Materials Science and Technology,
Nanjing University of Aeronautics and Astronautics,
Nanjing 210016, People's Republic of China
e-mail: yingang.wang@nuaa.edu.cn

layered composites with giant ME voltage coefficient by electro-deposition. These indicate that the ME effect can be improved by optimizing the configuration of ME composite. It is well known that the magnetostrictive–piezoelectric phase thickness ratio affects the ME performance of the plate laminated composite intensely [18, 23], but there is few report about that of cylindrical ME laminated composite. In this study, cylindrical Ni–PZT–Ni laminated composites were synthesized by electroless deposition and the ME performances of the composites with various magnetostrictive–piezoelectric phase thickness ratios were presented.

Experimental details

Prior to electroless deposition, the PZT rings (20 mm outer diameter, 18 mm inner diameter, and 5 mm height) were pretreated by the follow steps: (1) roughening, (2) sensitization, (3) activation, and (4) reduction. The PZT rings were immersed into a nickel sulfate bath for the deposition of Ni layers. The pretreatment parameters, bath composition, and operating parameters of electroless deposition were mentioned in details elsewhere [23]. The thickness of the Ni layers was controlled by the electroless deposition time and in this experiment the total thickness of the Ni layers was about 30, 50, and 60 μm, respectively. After the electroless deposition, the samples were poled with an electrical field of 30 kV cm^{-1} applied along the radial direction. Figure 1 shows the geometry arrangement of the cylindrical laminated ME composite.

For the ME measurement, a bias magnetic field H_{dc} (0–8000 Oe) was applied to the samples, superimposed with an ac field δH which was kept at 1.2 Oe in our experiment (1–120 kHz). The induced voltage δV was amplified and measured by an oscilloscope. The ME voltage coefficient α_E was calculated based on the equation $\alpha_E = \delta V/(t_{PZT}\ \delta H)$, where t_{PZT} is the thickness of PZT layer. Here two ME voltage coefficients, i.e., $\alpha_{E,A}$ and $\alpha_{E,V}$, were obtained according to two different conditions, magnetic fields along or vertical to the axis of the ring (Fig. 1).

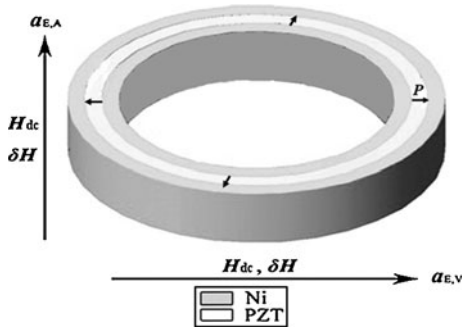

Fig. 1 The geometry arrangement of the cylindrical laminated ME composite

Results and discussion

Figure 2 shows the dependence of $\alpha_{E,A}$ on the bias magnetic field H_{dc} at $f = 1$ kHz for the Ni–PZT–Ni cylindrical laminated composites with various Ni layer thicknesses. It can be seen that the H_{dc} dependence of $\alpha_{E,A}$ is similar for all the samples. With the axial magnetic field increasing from zero, $\alpha_{E,A}$ increases first, reaches a maximum around H_{dc} = 270 Oe and then decreases rapidly. It nearly reduces to zero due to the magnetic saturation of the Ni layers when H_{dc} exceeds 2 kOe. From the inset, one can see that the peak values around H_{dc} = 270 Oe of the Ni–PZT–Ni cylindrical laminated composites with the total thickness of the Ni layers of 30, 50, and 60 μm are about 0.122, 0.166, and 0.178 V cm^{-1} Oe^{-1}, respectively. $\alpha_{E,A}$ at the same bias magnetic field increases as the Ni layer thickness increases, i.e., $\alpha_{E,A}$ increases as the ratio of Ni and PZT layer thickness increases because the thickness of PZT is the same for all the specimens. It is well known that the ME voltage coefficient goes up with the magnetostrictive–piezoelectric phase thickness ratio in plate ME laminated composites [18, 23]. We believe that this conclusion is also suitable for the cylindrical ME laminated composites.

Figure 3 shows the dependence of $\alpha_{E,V}$ on the bias magnetic field H_{dc} at $f = 1$ kHz for the Ni–PZT–Ni cylindrical laminated composites with various Ni layer thicknesses. Compared with the axial mode, as the vertical magnetic field increasing, there is a flat peak at high magnetic field (H_{m2} = 4100 Oe) besides the sharp peak around H_{m1} = 210 Oe. This is attributed to the more complex condition in the vertical mode which is discussed

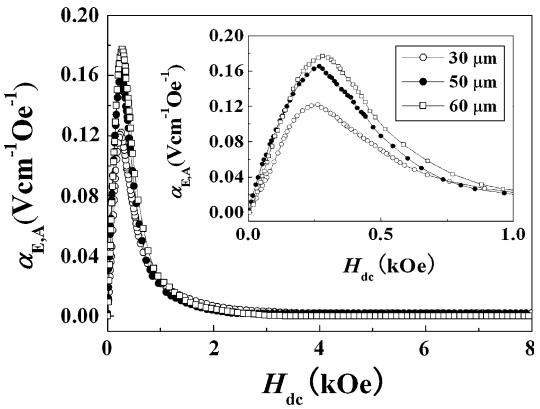

Fig. 2 The dependence of $\alpha_{E,A}$ on H_{dc} in the range of 0–8 kOe at $f = 1$ kHz for the Ni–PZT–Ni cylindrical laminated composites with various Ni layer thicknesses. The *inset* shows the dependence of $\alpha_{E,A}$ on H_{dc} in the range of 0–1 kOe

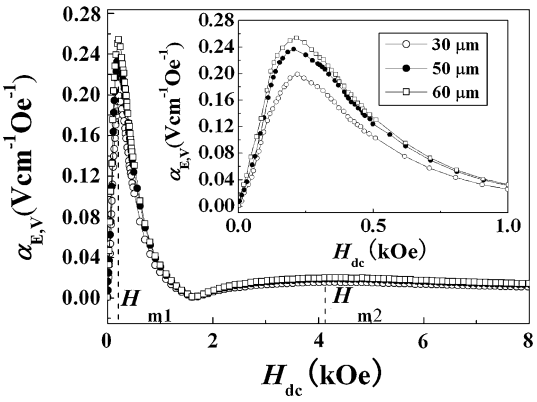

Fig. 3 The dependence of $\alpha_{E,V}$ on H_{dc} in the range of 0–8 kOe at $f = 1$ kHz for the Ni–PZT–Ni cylindrical laminated composites with various Ni layer thicknesses. The inset shows the dependence of $\alpha_{E,V}$ on H_{dc} in the range of 0–1 kOe

in details in Ref. [26]. The Ni–PZT–Ni cylindrical laminated composite in the vertical mode can be regarded as the combination of infinitesimal units with the magnetic fields acting along the thickness and length directions. The Ni layer thickness dependence of the ME voltage coefficient $\alpha_{E,V}$ is similar to that of $\alpha_{E,A}$. The inset shows that the peak values around $H_{dc} = 210$ Oe for samples with the total thickness of the Ni layers of 30, 50, and 60 μm are about 0.198, 0.236, and 0.254 V cm^{-1} Oe^{-1}, respectively. It can be seen that $\alpha_{E,V}$ is larger than $\alpha_{E,A}$ for individual samples. The infinitesimal units only suffer the magnetic field acting along the length direction in the axial mode, but they suffer the magnetic field acting along both the length direction and the thickness direction in the vertical mode. The addition of the magnetic field along the thickness direction in the vertical mode leads to higher ME voltage coefficient as reported in Ref. [26].

Figure 4 shows the frequency dependence of ME voltage coefficient for the Ni–PZT–Ni cylindrical laminated composites with various Ni layer thicknesses. For both $\alpha_{E,A}$ and $\alpha_{E,V}$, there is a sharp peak in resonance region and for samples with the Ni layer thicknesses of 30, 50, and 60 μm the resonant frequencies are about 49.9, 50.3, and 51.1 kHz, respectively. The resonant frequencies of both the axial and vertical modes are the same for individual samples, which is associated with the electromechanical resonance (EMR). The EMR frequency shifts to higher values with the Ni layer thickness increasing due to the fact that thicker Ni layer is more efficient in straining PZT and the structure becomes stiffer [25].

The resonant frequency of radial vibration mode for the Ni–PZT–Ni cylindrical laminated composite is given by

$$f_r = \frac{1}{\pi D}\sqrt{\frac{1}{\overline{\rho}\,\overline{s_{11}}}} \tag{1}$$

where f_r is the resonant frequency, D is the average diameter, and $\overline{\rho}$ is the average density. The equivalent elastic compliance $\overline{s_{11}}$ is given by

$$\overline{s_{11}} = \frac{s_{11}^{N} s_{11}^{P}}{v_N s_{11}^{P} + v_P s_{11}^{N}} \tag{2}$$

where v_N and v_P are the volume fractions of Ni and PZT layers, respectively, s_{11}^{N} and s_{11}^{P} are the respective elastic compliances of the Ni and PZT layers, respectively.

The following parameters for the Ni–PZT–Ni cylindrical laminated composite can be used:

$D = 19$ mm; $\overline{\rho} = 8 \times 10^3$ kg/m^3;

$s_{11}^{N} = 4.65 \times 10^{-12}$ m^2/N; $s_{11}^{P} = 15 \times 10^{-12}$ m^2/N.

The calculated resonant frequencies for the Ni–PZT–Ni cylindrical laminated composites with various Ni layer thicknesses are shown in Fig. 5. It can be seen that the calculated resonant frequency increases with the Ni layer thickness, which agrees with the experimental results.

The maximum of $\alpha_{E,A}$ is 0.724, 1.242, and 1.302 V cm^{-1} Oe^{-1}, while the maximum of $\alpha_{E,V}$ is 2.596, 3.136, and 3.256 V cm^{-1} Oe^{-1} when the Ni layer thickness is 30, 50, and 60 μm, respectively. It indicates that the difference between $\alpha_{E,A}$ and $\alpha_{E,V}$ for individual samples and the ME voltage coefficient dependence on the Ni layer thickness at resonant frequency coincide with those at low frequency discussed above. For the cylindrical Ni–PZT–Ni laminated composite with $t_{Ni}/(t_{Ni} + t_{PZT}) = 0.0566$ ($t_{PZT} = 1$ mm, $t_{Ni} = 60$ μm), the maximum ME coefficient is much higher

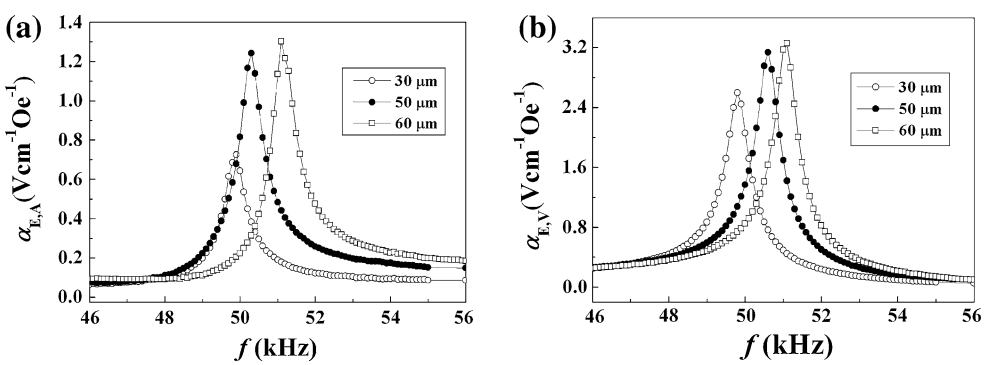

Fig. 4 The frequency dependence of ME voltage coefficient for the Ni–PZT–Ni cylindrical laminated composites with various Ni layer thicknesses. **a** $\alpha_{E,A}$ at $H_{dc} = 270$ Oe and **b** $\alpha_{E,V}$ at $H_{dc} = 210$ Oe

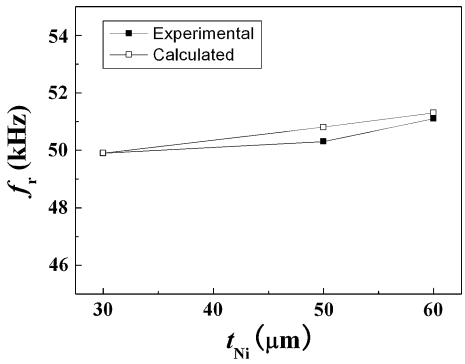

Fig. 5 The dependence of the resonant frequency f_r on the Ni layer thickness for the Ni–PZT–Ni cylindrical laminated composite. The *solid squares* are from experiments and the *hollow squares* are from the calculation based on Eq. 1. The *lines* are guides for the eye

than that of the plate Ni–PZT–Ni laminated composite, about 0.76 V cm^{-1} Oe^{-1}[23]. The higher ME coefficient of the cylindrical ME composite originates from the complex stress condition due to the self-bound effect of the circle. Only one piezoelectric mode of d_{31} contributes to ME coupling due to the free boundary condition of a plate composite, while the much higher d_{33} does not play a role. The stress condition in a cylindrical composite is more complex. When the Ni rings expands/shrinks in the magnetic fields, not only does the circumference increase/decrease, but the diameter also rises/reduces at the same time due to the self-bound effect of the circle. Thus each PZT infinitesimal unit will suffer from a radial force and a tangent force simultaneously due to the deformation of the Ni rings. Two piezoelectric modes of d_{33} and d_{31} in PZT contribute to the ME coefficient at the same time, so the cylindrical ME composite shows a higher ME voltage coefficient than that of the plate one[26].

Conclusion

The cylindrical Ni–PZT–Ni laminated composites with various magnetostrictive-piezoelectric phase thickness ratios were prepared by electroless deposition. $\alpha_{E,A}$, $\alpha_{E,V}$ and the resonant frequency all shift to higher values with the magnetostrictive–piezoelectric phase thickness ratio increasing. The maximum ME coefficient of the cylindrical Ni–PZT–Ni laminated composite is 3.256 V cm^{-1} Oe^{-1}, which is much higher than that of the plate laminated composite with the same magnetostrictive–piezoelectric phase thickness ratio. Electroless deposition is a convenient method to fabricate ME laminated composites with complex structures and optimizing the structure can provide proper resonant frequency and stronger ME effect.

Acknowledgements This study is supported by the Natural Science Foundation of Jiangsu Province of China (Grant No. BK2010505) and the Scientific Research & Innovation Foundation of NUAA. K. B. would like to acknowledge support from the Funding of Jiangsu Innovation Program for Graduate Education (Grant No. CX10B_099Z).

References

1. Fiebig M (2005) J Phys D Appl Phys 38:R123
2. Nan C, Bichurin M, Dong S, Viehland D, Srinivasan G (2008) J Appl Phys 103:031101
3. Landau L, Lifshitz E (1960) Electrodynamics of continous media. Pergamon, Oxford
4. Astrov D (1960) Sov Phys JETP 11:708
5. Boomgaard J, Born R (1978) J Mater Sci 13(7):1538. doi:10.1007/BF00553210
6. Boomgaard J, Van Run A, Van Suchtelen J (1976) Ferroelectrics 10(1):295
7. Ryu J, Priya S, Uchino K, Kim H (2002) J Electroceram 8(2):107
8. Van den Boomgaard J, Terrell D, Born R, Giller H (1974) J Mater Sci 9(10):1705. doi:10.1007/BF00540770
9. Van Suchtelen J (1972) Philips Res Rep 27:28
10. Bai W, Meng X, Yang J, Lin T, Zhang Q, Ma J, Sun J, Chu J (2009) J Phys D Appl Phys 42:145008
11. Ryu J, Carazo A, Uchino K, Kim H (2001) Jpn J Appl Phys 40(8):4948
12. Mori K, Wuttig M (2002) Appl Phys Lett 81(1):100
13. Nan C, Cai N, Shi Z, Zhai J, Liu G, Lin Y (2005) Phys Rev B 71(1):14102
14. Nan C, Liu L, Cai N, Zhai J, Ye Y, Lin Y, Dong L, Xiong C (2002) Appl Phys Lett 81(20):3831
15. Wan J, Liu J, Chand H, Choy C, Wang G, Nan C (2003) J Appl Phys 93(12):9916
16. Dong S, Zhai J, Xing Z, Li J, Viehland D (2007) Appl Phys Lett 91:022915
17. Pan D, Bai Y, Chu W, Qiao L (2007) Smart Mater Struct 16:2501
18. Pan D, Bai Y, Chu W, Qiao L (2008) J Phys Condens Matter 20:025203
19. Pan D, Zhang S, Volinsky A, Qiao L (2008) J Phys D Appl Phys 41:195004
20. Nan C, Liu G, Lin Y (2003) Appl Phys Lett 83:21
21. Liu G, Nan C, Cai N, Lin Y (2004) J Appl Phys 95:2660
22. Barker B (1981) Surf Technol 12(1):77
23. Bi K, Wang Y (2010) Solid State Commun 150(5–6):248
24. Bi K, Wang Y, Wu W, Pan D (2010) J Phys D Appl Phys 43:132002
25. Wan J, Li Z, Wang Y, Zeng M, Wang G, Liu J (2005) Appl Phys Lett 86:202504
26. Pan D, Bai Y, Chu W, Qiao L (2008) J Phys D Appl Phys 41:022002
27. Pan D, Bai Y, Volinsky A, Chu W, Qiao L (2008) Appl Phys Lett 92:052904
28. Pan D, Zhang S, Volinsky A, Qiao L (2008) J Phys D Appl Phys 41:205008